International Journal of the Physical Sciences Vol. 6(11), pp. 2593-2606, 4 June, 2011
Available online at http://www.academicjournals.org/IJPS
DOI: 10.5897/IJPS11.367
ISSN 1992 - 1950 ©2011 Academic Journals

Review

Reducing the peak to average power ratio in OFDM systems

Sabhyata Uppal[1*] and Sanjay Sharma[2]

[1]UIET, Panjab University, Chandigarh, India.
[2] Thapar University, Patiala, India.

Accepted 31 March, 2011

High peak to average power ratio of the transmit signal is a major drawback of OFDM systems. After defining the PAPR and analyzing its statistical properties, some of the most representative PAPR-reduction techniques available in the literature are reviewed in detail. Several methods have been proposed to reduce the peak power of OFDM signals. In this paper the effectiveness of some recently proposed methods has been evaluated.

Key words: PAPR, OFDM, amplitude clipping, SLM.

INTRODUCTION

One of the major obstacles to the practical implementation of a multicarrier system is represented by the relatively high peak-to-average power ratio (PAPR) of the transmitted waveform. Recalling that the OFDM signal is a superposition of *N* sinusoids modulated by possibly coded data symbols, the peak power can theoretically be up to *N* times larger than the average power level. This fact poses two different problems. The first one is related to the A/D and D/A converters, which must be equipped with a sufficient number of bits to cover a potentially broad dynamic range. The second difficulty is that the transmitted signal may suffer significant spectral spreading and in-band distortion as a consequence of intermodulation effects induced by a non-linear power amplifier (PA). One possible method to circumvent this problem is the use of a large power backoff which allows the amplifier to operate in its linear region. However, this results into considerable power efficiency penalty, which translates into expensive transmitter equipment and reduced battery lifetime at the user's terminal. It is thus of interest to look for some efficient schemes that can reduce the occurrence of large signal peaks at the input of the PA so as to minimize the detrimental effects of non-linear distortions without sacrificing the power efficiency.

*Corresponding author. E-mail: sabhyata2@gmail.com.

OFDM signal and PAPR

The continuous-time baseband representation of an OFDM signal with N subcarriers is given by,

$$s(t) = \frac{1}{\sqrt{N}} \sum_{n=0}^{N-1} c(n)\, {}^{ej2\pi n f_{cs} t},\ 0 \le t < T \tag{1}$$

where *c(n)* is the data symbol transmitted onto the *n*th subchannel, f_{cs} denotes the subcarrier spacing and T = 1/ f_{cs} is the data block duration (excluded the cyclic prefix). As indicated in Equation (1), *s(t)* is the superposition of *N* modulated complex sinusoidal waveforms, each corresponding to a given subcarrier. In the extreme situation where all sinusoids interfere constructively, their sum will result into a large signal peak that greatly exceeds the average power level. Furthermore, assuming that N is adequately large, we can reasonably approximate s(t) as a Gaussian random process by virtue of the central limit theorem (CLT). As shown later, this assumption plays an important role in the statistical characterization of the signal amplitude. After baseband processing, *s(t)* is up-converted to a higher carrier frequency f_c. The resulting RF waveform is expressed by

$$S_{RF}(t) = \mathrm{Re}\left\{ s(t) e^{j2\pi f_c t} \right\} \tag{2}$$

which represents the actual input to the PA. Thus, strictly speaking the PAPR should be defined over $s_{RF}(t)$ rather than over $s(t)$. However, since this approach would lead to some mathematical complications, it is a common practice to measure the PAR at baseband. This procedure provides accurate results as long as $fc >> 1/T$, a condition that is always met in all practical systems.

With the above assumption, the continuous-time PAPR is defined as

$$\gamma_c \stackrel{def}{=} \frac{\max_{0 \le t < T} |s(t)|^2}{E\{|s(t)|^2\}} \tag{3}$$

and is sometimes referred to as the peak-to-mean envelope power (PMEPR) [Sharif et al., 2003; Tarokh and Jafarkhani, 2000]. Without loss of generality, one can normalize s(t) such that $E\{|s(t)|^2\} = 1$. In this case γ_c reduces to

$$\gamma_c = \frac{\max_{0 \le t < T} |s(t)|^2}{E\left\{|s(t)|^2\right\}} \tag{4}$$

In principle, the maximum of $|s(t)|^2$ can be computed by setting its derivative to zero. Unfortunately, this operation is not trivial since the derivative is a sinusoidal function and its roots cannot easily be found. To overcome this difficulty, it is expedient to replace the continuous-time waveform $s(t)$ by its samples $\{s_k^{(L)}\}$ taken at some rate L/T_s, where $Ts = T/N$ while L is a suitable integer which is commonly referred to as *oversampling factor*. This leads to the definition of the following *discrete-time* PAPR.

$$\gamma_d \stackrel{def}{=} \max_{0 \le k \le LN-1} |s_k^{(L)}|^2 \tag{5}$$

where $s_k^{(L)}$ is obtained after setting $t = kT_s/L$ into Equation (1), that is,

$$s_k^{(L)} = \frac{1}{\sqrt{N}} \sum_{n=0}^{N-1} c(n) e^{j2\pi nk/LN}, \quad 0 \le k \le LN - 1 \tag{6}$$

Inspection of Equation (5) reveals that the discrete-time PAPR is computed through a numerical search over the set $\{|S_k^{(L)}|^2; k = 0, 1, \ldots, NL-1\}$, thereby avoiding the need for solving highly non-linear equations. Moreover, comparing Equations (4) and (5) it is easily seen that γ_d approaches γ_c as L grows large. For this reason, γ_d is normally employed as a practical metric for evaluating the performance of PAPR-reduction techniques.

Statistical properties of PAPR

The statistical properties of the PAPR are normally given in terms of the corresponding CCDF. From the central limit theorem we know that the real and imaginary parts of the time-domain samples $\{S_k^{(L)}\}$ can reasonably be approximated as statistically independent Gaussian random variables with zero mean and variance $\sigma^2 = 1/2$. Figure 1 shows the transmitter CCDF downlink and uplink. Figure 2 depicts the corresponding transmitter relative constellation error (RCE).

Distribution of OFDM signal

Figure 3 shows the individual time domain QPSK modulated subcarriers for N= 8 and their sum in terms of its continuous time version. The PAPR characteristics of the OFDM signal is obvious from Figure 3. In general we expect the PAPR to become significant as N increases. Figure 4 shows the distributions including the real and imaginary parts for N=16, which again illustrates the PAPR characteristics of OFDM signal.

Downlink BER performance is evaluated in an AWGN channel as shown in Figure 5. Figure 6 depicts the uplink BER and PER on a fading channel.

Amplitude clipping

The simplest approach to limit the amplitude peaks in a multicarrier wave-form is to deliberately clip the signal before amplification [O'Neill and Lopes, 1995]. This operation is normally accomplished at baseband using a soft envelope limiter.

The distortion caused by the clipping process is mathematically expressed as

$$d(t) = y(t) - s(t) \tag{7}$$

and is viewed as an additional source of noise. Since the derivative of $d(t)$ exhibits discontinuities at the clipping instants, its bandwidth is theoretically infinite. This means that in general amplitude clipping gives rise to in-band distortion as well as out-of-band emission. The former degrades the bit-error-rate (BER) performance while the latter reduces the spectral efficiency of the communication system. Filtering after clipping can reduce out-of-band radiation to a large extent, but may also produce some peak re-growth in the filtered signal [Li and Cimini, 1998].

Clipping and filtering of oversampled signals

In practical applications clipping and filtering is performed digitally (that is before D/A conversion) on an

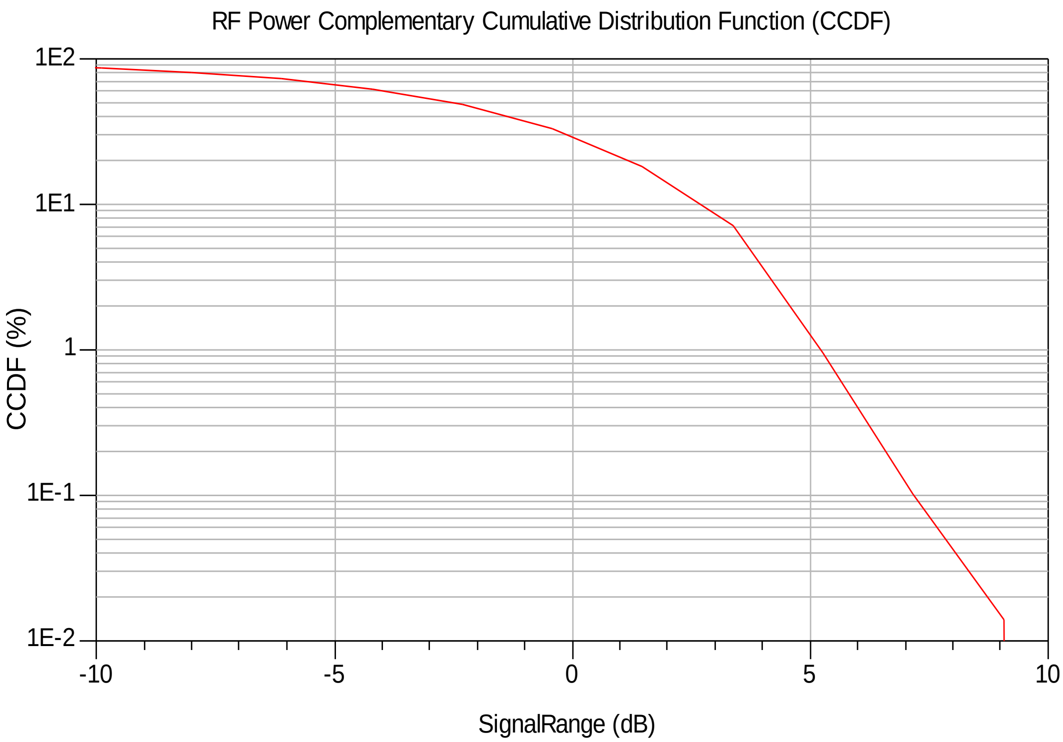

PeakPower_dBm	MeanPower_dBm	RF_Peak_to_Avg_dB
-0.449	-9.505	9.056

Figure 1. Transmitter CCDF downlink and uplink.

EVM (or RCE)

RCE_dB	RCErms_percent
-36.661	1.469

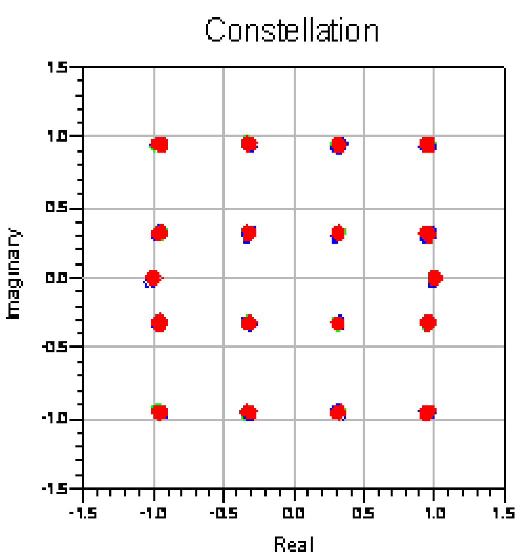

Specification Requirement

The relative constellation RMS error, averaged over subcarriers, OFDM frames, and packets, shall not exceed a burst profile dependent value according to Table below
(as defined in section 8.3.10.1.2, IEEE Std 802.16-2004)

Burst type	Relative Constellation Error (dB)
BPSK-1/2	-13.0
QPSK-1/2	-16.0
QPSK-3/4	-18.5
16-QAM-1/2	-21.5
16-QAM-3/4	-25.0
64-QAM-2/3	-28.5
64-QAM-3/4	-31.0

Figure 2. Corresponding transmitter relative constellation error (RCE).

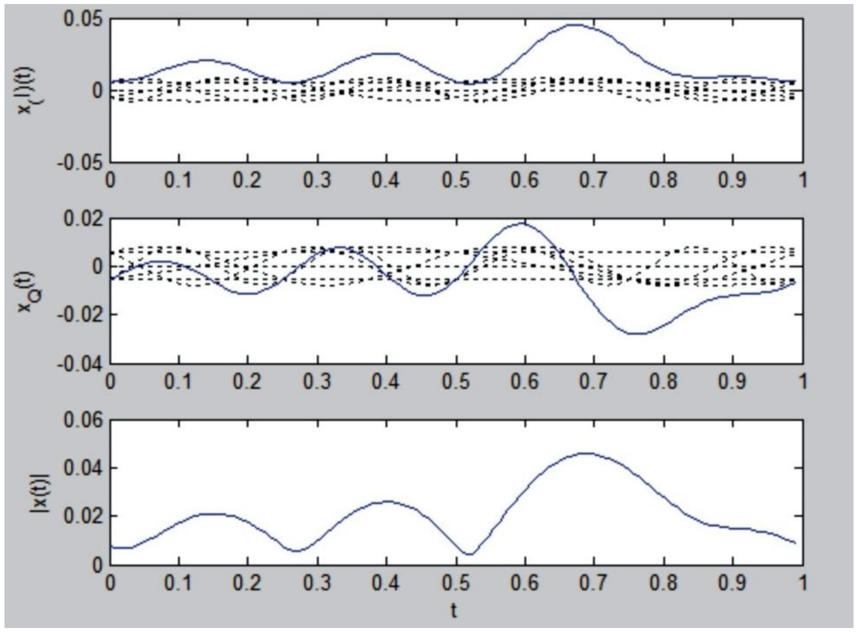

Figure 3. Individual time domain QPSK modulated subcarriers.

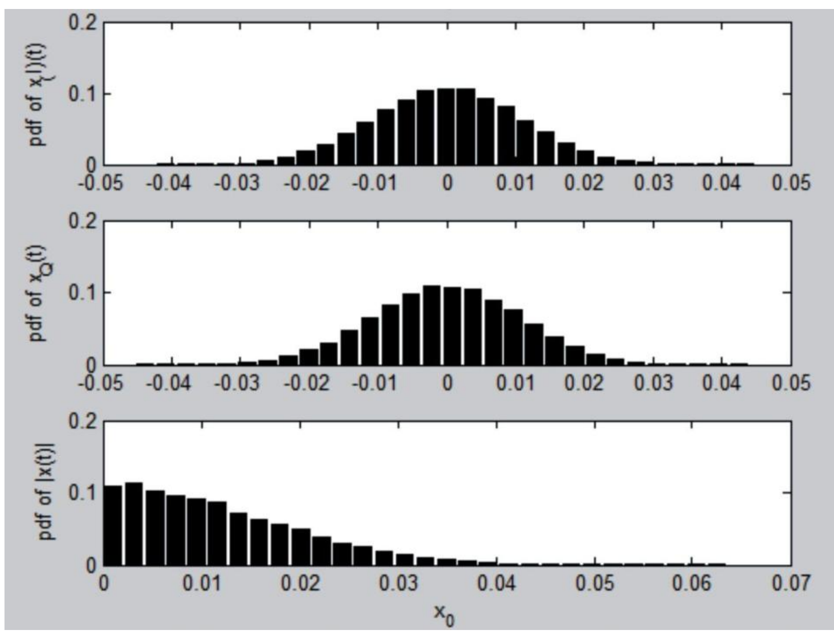

Figure 4. Distributions including the real and imaginary parts for N=16.

oversampled version of the OFDM signal [Han and Lee, 2004]. Letting J ≥ 1 be the employed oversampling factor, we denote,

$$s(k) = \frac{1}{\sqrt{N}} \sum_{n=0}^{N-1} c(n)\, e^{j2\pi nk/JN}, \quad 0 \le k \le JN-1 \qquad (8)$$

the sample of s(t) corresponding to a given block of data c = [c(0), c(1), …., c(N-1)]^T. Note that J should not be confused with parameter L defined earlier . Indeed, the former is the oversampling factor that is actually used in OFDM transmitter to execute clipping and filtering operations, while the latter is just a parameter employed in computer simulations for PAPR measurements [Ochiai and Imai, 2000; Ochiai and Imai, 2002].

As illustrated in Figure 7, the oversampled data sequence, *s* = [*s*(0), *s*(1),…, *s*(*JN*-1)]^T, can be efficiently generated as the IDFT of the Zero-padded data block

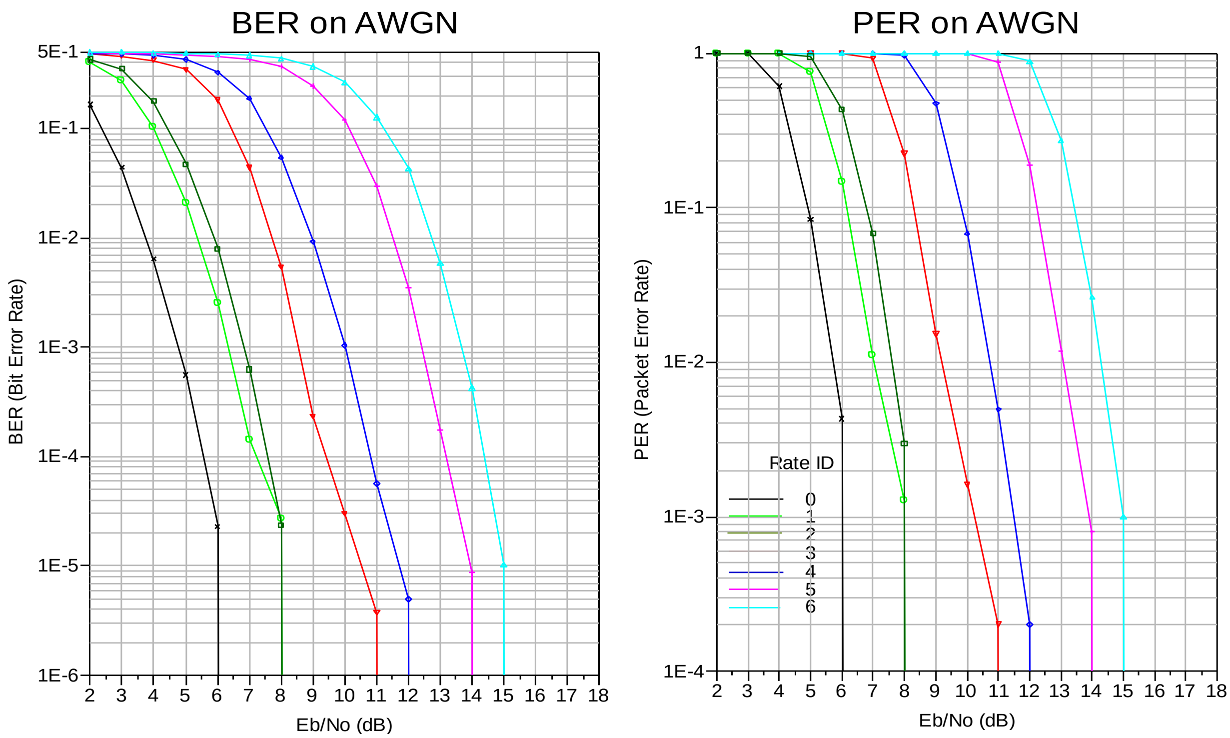

Figure 5. Downlink BER performance evaluated in an AWGN channel.

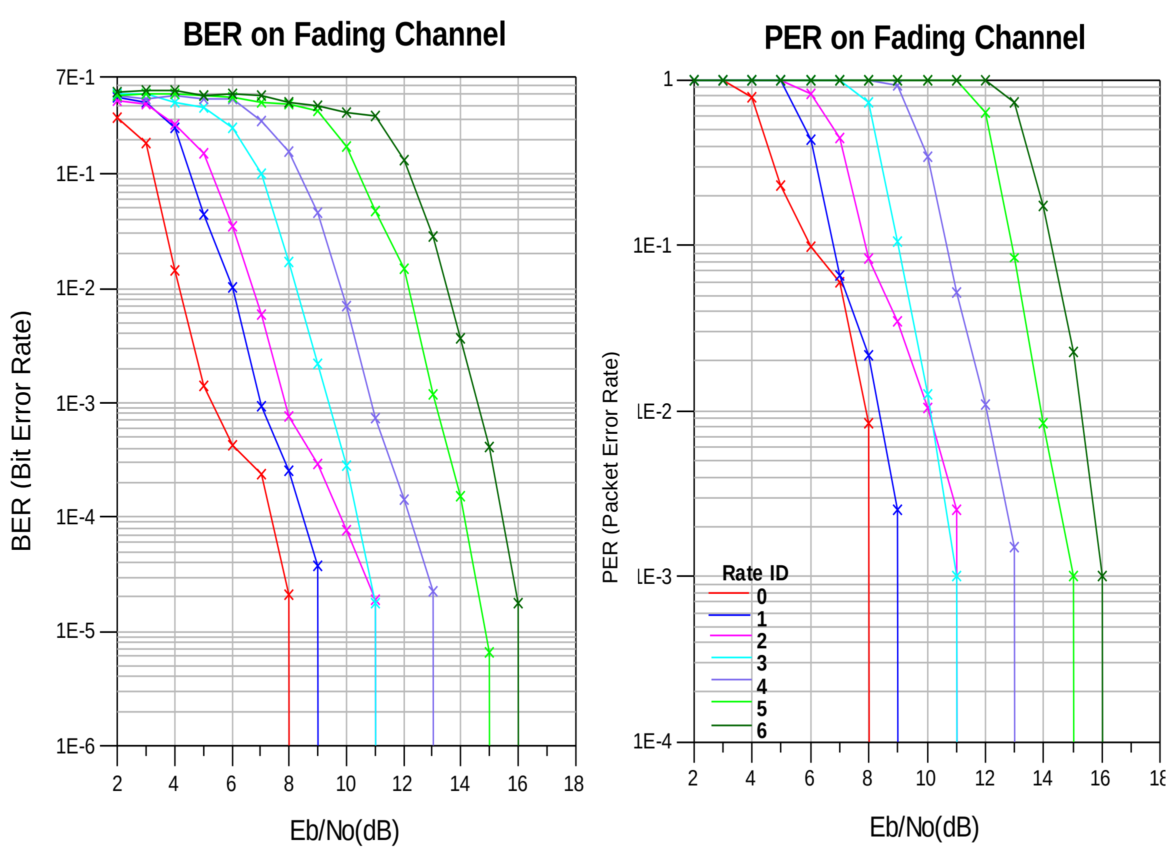

Figure 6. Uplink BER & PER on a fading channel.

$c^{(ZP)}$, which is obtained by extending c with *(J – 1) N* Zeros.

$$c^{(ZP)} = [c(0),\ c(1),\ ....,\ c(N-1), \underbrace{0,\ 0,\ ....,\ 0}_{(J-1)N}]^{T} \qquad (9)$$

Each sample s(k) is then clipped by a soft envelope limiter. Let $p_k e^{j\varphi k}$ be the representation of *s(k)* in polar coordinates, the output from the limiter is given by

$$\tilde{s}(k) = \begin{cases} s(k), & if\ \rho_k \le A \\ Ae^{j\varphi k}, & if\ \rho_k \le A \end{cases} \qquad (10)$$

It is a common practice to normalize the clipping level A to the root-mean-square (rms) value of the input signal. This results into the following clipping ratio (CR)

$$\mu = \frac{A}{\sqrt{P_{in}}} \qquad (11)$$

Where P_{in} = E{|s(k)|^2} is the average power of the unclipped samples.

As is intuitively clear, the clipping process leads to a certain reduction of the output power. If the OFDM signal can be modeled as a zero-mean circularly symmetric complex Gaussian process, the amplitude p_k is Rayleigh distributed and the average power of the clipped samples turns out to be

$$P_{out} = (1 - e^{-\mu^2})\ P_{in} \qquad (12)$$

Note that the difference between Pout and Pin reduces as μ grows large and becomes zero when μ = ∞, which corresponds to an ideal system without clipping.

As mentioned earlier, in general the power spectral density (PSD) of the non-linear distortion introduced by the amplitude limiter has a theoretically infinite bandwidth. Hence, aliasing will occur if clipping is carried out on the samples {*s*(*k*)} rather than on the continuous-time signal *s(t)*. In particular, when clipping is done at the Nyquist rate (*J* = 1), the spectrum of the resulting distortion is folded back into the signal bandwidth. This gives rise to considerable in-band distortion, with ensuing limitations of the error-rate performance. Furthermore, extensive simulations indicate that the PAPR reduction capability of Nyquist-rate clipping is not so significant due to considerable peak re-growth after D/A conversion [Ochiai and Imai, 2000; Ochiai and Imai, 2002]. As a result, clipping is normally performed on an oversampled version of the OFDM signal (*J* > 1). The oversampled approach has the advantage of reducing in-band distortion and peak re-growth to some extent, but inevitably generates out-of-band radiation that must be removed in some way. Clipping at Nyquist rate considerably reduces the PAPR of the transmitted signal as compared to a system without clipping. However, much better results are obtained if clipping is executed on the oversampled waveform. In particular, a PAPR reduction of approximately 2 dB is achieved when *J* is increased from 1 to 4. Clearly, this advantage comes at the expense of a higher computational complexity due to the larger dimension of the IDFT unit in Figure 3 and the need for filtering the signal after clipping. Theoretical analysis [Sharif and Khalaj, 2001] and computer simulations [Li and Cimini, 1998] indicate that in many cases a good trade-off between performance and complexity is obtained with an oversampling factor of 4. Repeated clipping and filtering operations can also be used to further reduce the overall peak re-growth after D/A conversion [Armstrong, 2002].

Selected mapping (SLM) technique

One possible approach of PAPR control in multicarrier systems is based on the idea of mapping the data block c = [c(0), c(1),…,c(N – 1)T into a set of adequately different signals and then choosing the most favorable one for transmission. This technique is called selected mapping (SLM) and its main concept is shown in Figure 8.

As is seen, the transmitter generates a number Q of candidate data blocks Cq = [$c_q(0)$, $c_q(1)$,…$c_q(N – 1)]^T$ (q = 1, 2, …, Q) using some suitable algorithm. Each block has length N and conveys the same information as the original data sequence c. The latter is normally included into the set of candidate block by letting c_1 = c. After transforming all blocks c_q in the time-domain, the exhibiting the lowest PAPR is selected for transmission.

Since the PAPR of the continuous-time waveform cannot precisely be computed from its Nyquist-rate samples, each candidate block is padded with (L – 1) N zeros and fed to a LN – point IDFT unit. This provides Q oversampled sequences $S_q^{(L)}$ (q = 1, 2, …., Q) with entries

$$s_{q,k}^{(L)} = \frac{1}{\sqrt{N}} \sum_{n=0}^{N-1} c_q(n)\ e^{j2\pi nk/LN},\quad 0 \le k \le NL-1 \qquad (13)$$

and characterized by the following discrete time PAPRs.

$$\gamma_q = \frac{\max_{0\le k \le LN-1} \left| s_{q,k}^{(L)} \right|^2}{\hat{P}_q}, \qquad q = 1, 2, ..., Q. \qquad (14)$$

With

$$\hat{P}_q = \frac{1}{N} \sum_{n=0}^{N-1} |\ c_q(n)\ |^2 \qquad (15)$$

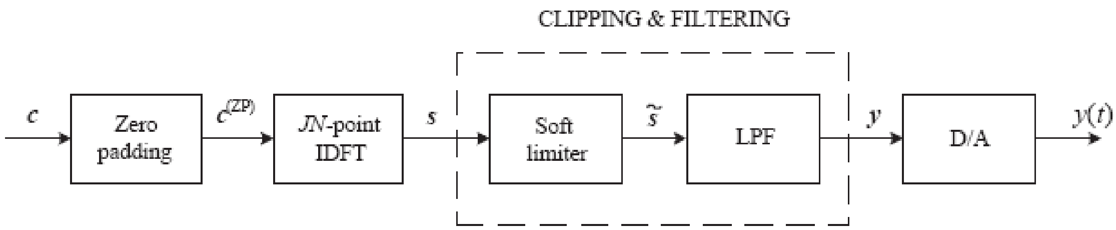

Figure 7. Clipping and filtering operations on the oversampled OFDM signal.

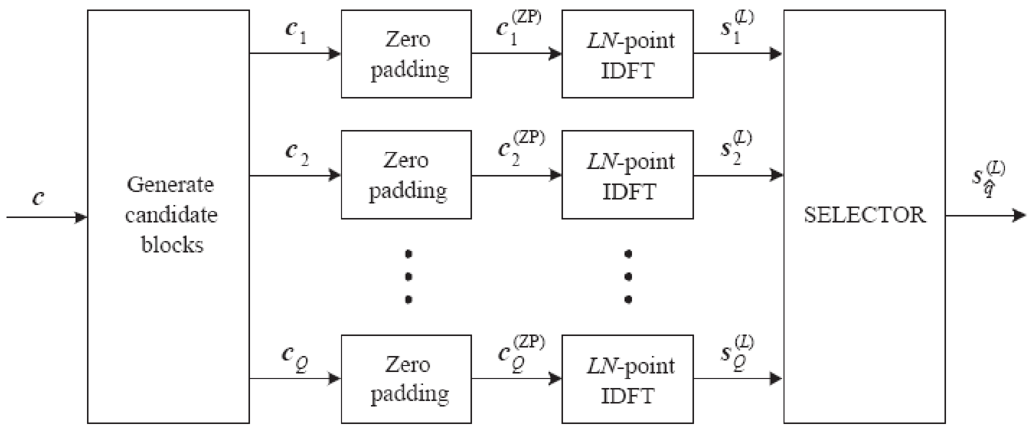

Figure 8. Block diagram of the SLM technique.

As mentioned before, setting L = 4 is sufficient to capture the peaks of the continuous time waveform.

The selector in Figure 7 computes the quantities γ_q and chooses the sequence $S_q^{(L)}$ such that,

$$\hat{q} = \arg \min_{1 \le q \le Q} \{\gamma_q\} \tag{16}$$

The selected sequence is then passed to the D/A converter and the corresponding waveform is finally launched over the channel after up-conversion and power amplification.

To better illustrate the PAPR reduction capability of the SLM technique, we denote $F_q(\gamma) = \Pr\{\gamma_q \ge \gamma\}$ the CCDF of γ_q and observe that

$$F_{\hat{q}}(\gamma) = \Pr\left\{\bigcap_{q=1}^{Q} (\gamma_q \ge \gamma)\right\} \tag{17}$$

Since γ_q is the minimum of the set $\{\gamma_q\}$. If the candidate sequence $S_q^{(L)}$ is sufficiently “different”, the random variables γ_q may be considered as nearly independent and Equation (17) reduces to

$$F_{\hat{q}}(\gamma) = \prod_{q=1}^{Q} F_q(\gamma) \tag{18}$$

Figure 9 illustrates function $F_{\hat{q}}(\gamma)$ for N = 256 and some values of Q. The results are derived analytically under the simplifying assumption that each factor $F_q(\gamma)$ in Equation (18) can be expressed as indicated in Equation (6). In this case we have

$$F_{\hat{q}}(\gamma) = [1 - (1 - e^{-\gamma})^{\alpha N}]^{Q} \tag{19}$$

with α = 2.8. As expected, the amount of PAPR reduction depends on the number Q of candidate sequences. We see that significant gains are achieved in passing from Q = 1 to Q = 4, while only marginal improvements are observed with higher values of Q.

Coding

It is a well recognized fact that the frequency diversityoffered by the multipath channel cannot be fully exploited in OFDM systems, without employing some form of channel coding. A natural question is whether the redundancy introduced by channel coding can be exploited not only for error correction purposes, but also as a means for minimizing the PAPR of the transmitted waveform. The possibility of using block coding for PAPR reduction was originally proposed in Jones et al. (1994],

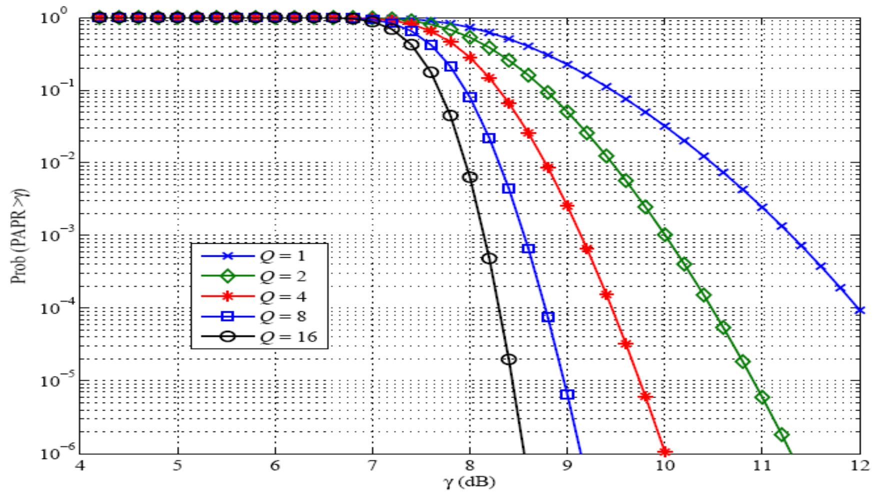

Figure 9. Function F $\hat{q}$ (γ) for different values of Q.

Table 1 . PAPR γ_d of BPSK modulated codewords with N = 4.

Code words				BPSK symbols				PAPR (dB)
b(0)	b(1)	b(2)	b(3)	c(0)	c(1)	c(2)	c(3)	γ_d
0	0	0	0	1	1	1	1	6.02
1	0	0	0	-1	1	1	1	2.32
0	1	0	0	1	-1	1	1	2.32
1	1	0	0	-1	-1	1	1	3.72
0	0	1	0	1	1	-1	1	2.32
1	0	1	0	-1	1	-1	1	6.02
0	1	1	0	1	-1	-1	1	3.72
1	1	1	0	-1	-1	-1	1	2.32
0	0	0	1	1	1	1	-1	2.32
1	0	0	1	-1	1	1	-1	3.72
0	1	0	1	1	-1	1	-1	6.02
1	1	0	1	-1	-1	1	-1	2.32
0	0	1	1	1	1	-1	-1	3.72
1	0	1	1	-1	1	-1	-1	2.32
0	1	1	1	1	-1	-1	-1	2.32
1	1	1	1	-1	-1	-1	-1	6.02

where only code words exhibiting the lowest PAPR are selected for transmission while discarding all the others. Table 1 illustrates the highly-cited example given in Jones et al. (1994], where the discrete-time PAPR is listed for all possible data blocks in a BPSK-OFDMsystem with N = 4 subcarriers and oversampling factor L = 4.

We see that four data blocks are characterized by a maximum PAPR of 6:02 dB and another set of four blocks results into a PAPR of 3:72 dB. Clearly, using a suitable coding scheme that avoids transmitting these sequences helps to reduce the PAPR of the transmitted signal. In the particular example shown in Table 1, this goal is achieved with an odd parity check code of rate 3/4 where the first three elements $b(0)$; $b(1)$; $b(2)$ in each codeword represents the information bits while the fourth element is computed as $b(3) = b(0) \oplus b(1) \oplus b(2) \oplus 1$, with $\oplus$ denoting the arithmetic addition in the binary Galois field. In this way the PAPR becomes 2.32 dB for all codewords, thereby leading to a reduction of 3.70 dB with respect to the uncoded system. It is shown in Jones et al. [1994] that higher gains of 4.58 and 6.02 dB are possible in case of N = 8 subcarriers using coding schemes with rates 7=8 and 3=4, respectively. Clearly, these benefits are achieved at the price of some penalty in terms of spectral efficiency due to the inherent

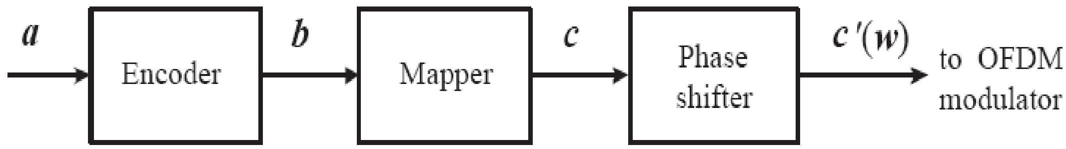

Figure 10. Coding and phase rotation for simultaneous error control and PAPR reduction.

redundancy introduced in the transmitted signal. Note that the latter is only exploited for PAPR reduction purposes rather than to protect information against channel impairments. In addition the method in Jones et al. [1994] becomes impractical for large values of *N* since the best codes can only be found through an exhaustive search and prohibitively large look-up tables are required for the encoding and decoding operations.

A more sophisticated approach proposed by Jones and Wilkinson in [1996] relies on the design of combined coding schemes for *simultaneous* error control and PAPR reduction. This solution employs conventional linear block codes to achieve the desired level of error protection and the code redundancy is subsequently exploited to minimize the PAPR. The basic idea behind this method is sketched in Figure 10. Let ν be the number of points in the employed constellation and assume that a (N ν, k) binary block code has been chosen for its correction property. As is seen, a block a of k information bits is first transformed into a vector b of Nν coded bits. The latter is next divided into N adjacent segments of length ν, where each segment is independently mapped onto a modulation symbol c(n). This produces a codeword c = {c(0), c(1),…c(N – 1)} of length N for each block of k information bits. We denote C = {c_m; m = 1, 2, 3, …, 2^k} the set of all possible codewords. Then, in an attempt of reducing the PAPR, the codewords are element-wide multiplied by a same rotating vector

$$w = \{e^{j\psi(0)}, e^{j\psi(1)}, ..., e^{j\psi(N-1)},]^T,$$

where the phase shifts $\{\psi(n)\}$ vary in the compact set [0, 2π] x [0, 2π] x …. X [0, 2π]. The rotated version of C_m is denoted c'_m(w) and reads

$$c`_m(w) = \{c_m(0)e^{j\psi(0)}, c_m(1)e^{j\psi(1)}, ..., c_m(N-1)e^{j\psi(N-1)}\} \quad (20)$$

Since distances among codewords remain unchanged after rotation, the new code C′(w) = {c'_m (w); m = 1, 2, 3, …, 2^k} has the same error correction capability as the original code C. However, it may exhibit a lower PAPR if the phase shifts are suitably chosen. Hence, for a given code C, the problem is to find an optimal vector

$\hat{w} = [e^{j\psi(0)}, e^{j\psi(1)}, ..., e^{j\psi(N-1)},]^T$ such that

$$\hat{w} = \arg\min_{w}\{\mathrm{PAPR}[C`(w)]\} \quad (21)$$

where PAPR[C'(w)] is defined as

$$PAPR[C`(w)] = \max_{c`_m(w) \in C`(w)} \{\mathrm{PAPR}[c'_m(w)]\} \quad (22)$$

with PAPR[c'_m(w)] denoting the PAPR of the waveform associated to the *mth* rotated codeword c'_m(w).

It is worth nothing that in this way PAPR reduction comes for free since, as mentioned previously, both *C* and *C'(w)* are perfectly equivalent in terms of error rate performance and decoding complexity. At the receive side, the phase shifts introduced by $\hat{w}$ can easily be compensated for by appropriate counter-rotation of the DFT output. For this purpose, $\hat{w}$ must be known to the receiver.

The main drawback of the described approach is the heavy computational load that is required to solve the optimization problem Equation (21). An algorithm for finding the optimum rotation vector is discussed in Jones and Wilkinson [1996] under the assumption that the phase shifts belong to a finite set Ψ = {2πl/W; l = 0, 1, ….., W - 1}. Unfortunately, this method is only applicable to relatively short codes because of the huge complexity involved in computing the PAR of all phase-shifted codewords. A computationally efficient solution to this problem is outlined in [Tarokh and Jafarkhani, 2000], where a simplified method is proposed to identify codewords characterized by the highest PAPR and a gradient-based iterative minimization technique is next used to search for the optimum rotation vector.

A third approach for the design of low-PAPR coding schemes was motivated by the observation that the PAPR of an OFDM signal is at most 3 dB if the modula tion sequence is constrained to be a member of a Golay complementary pair [Golay, 1961; Popovic, 1991]. For a long time these sequences were not recognized to possess sufficient structure to form a practical coding scheme until a theoretical connection has been established between them and the first and second-order Reed-Muller codes [Davis and Jedwab, 1997]. This connection offers the opportunity to combine the error correcting capability of classical Reed-Muller codes with the attractive PAPR control property of Golay complementary sequences. Further improvements to this approach are found in Davis and Jedwab [1999], where a range of flexible coding schemes using binary, quaternary and higher order modulations has been designed to

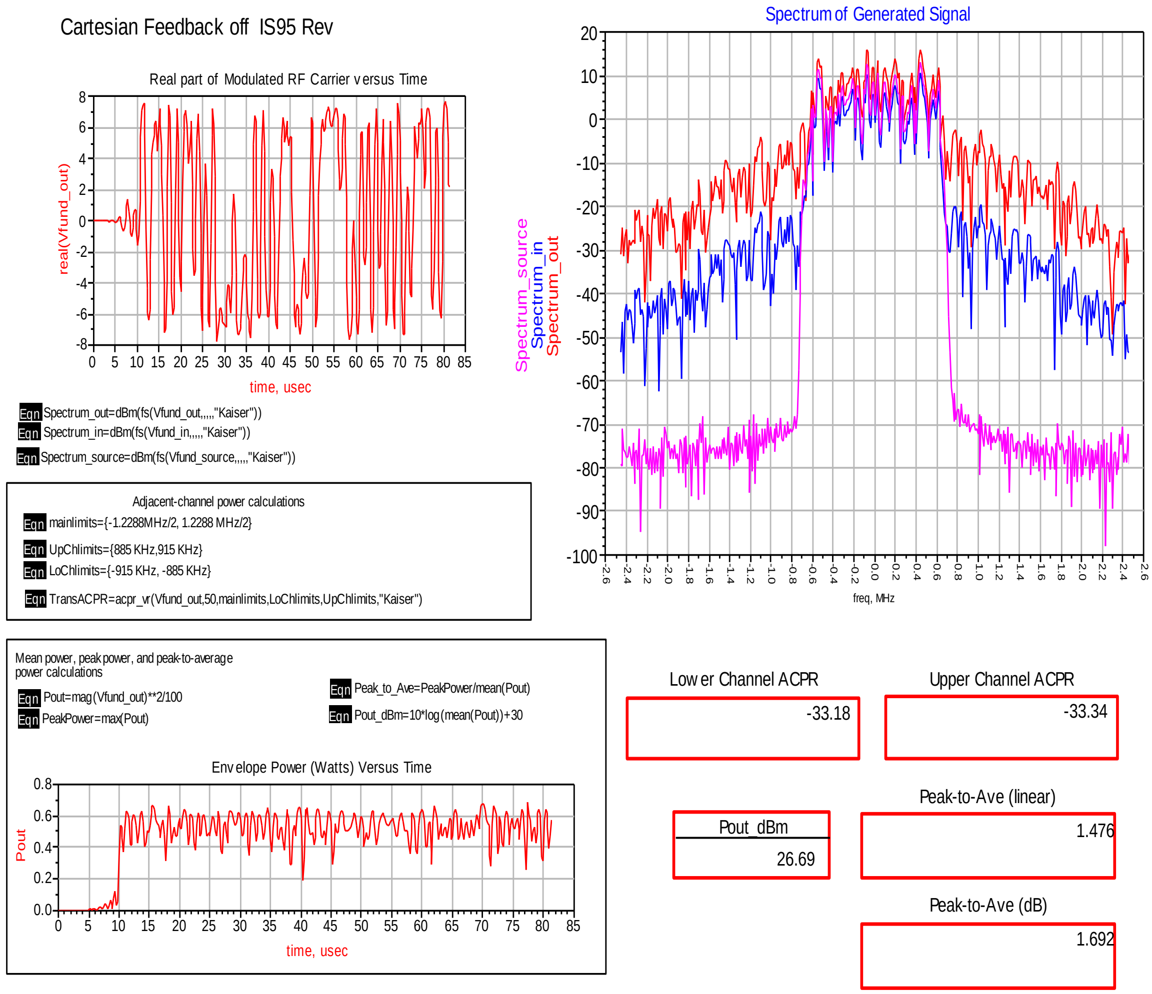

Figure 11. Open loop.

achieve desired tradeoffs in terms of PAPR control, spectral efficiency and error-correcting capability. Computationally efficient decoding algorithms have also been developed based on the fast Hadamard transform (FHT). A unified theory linking Golay complementary sets of polyphase sequences and Reed-Muller codes has been presented by Paterson in [Paterson, 2000] and exploited to design a broad range of coding option employing high-order modulations. Unfortunately, the usefulness of all these techniques is somewhat limited by the fact that they can only be applied to multicarrier systems with a small number of subcarriers in order to keep the computational complexity to a tolerable level. One possible advantage is that no side information is required at the receiver to recover the transmitted data symbols.

Cartesian Feedback

The basic concept of closed loop feedback control is well known as it has been widely applied in a variety of applications that use different FB configurations. In the basic Cartesian loop feedback (CLFB) scheme, the signal is separated into in-phase and quadrature components which allow the correction of amplitude gain into in-phase shift simultaneously. The HPA output is sampled and then the low pass feed-back components perform an additive pre-distortion of the I-Q components at each input adder, subtracting from the original input the orthogonal error signals introduced by the nonlinearity. A remarkable advantage of this kind of linearizer is that both the signal modulation and amplification processes are jointly considered in the linearization procedure. This means that non-linear distortions originating in sources external to the HPA (at the mixers, for instance) are also compensated. The results are depicted in Figures 11- 14.

Conclusion

Various techniques for reducing the PAPR in OFDM

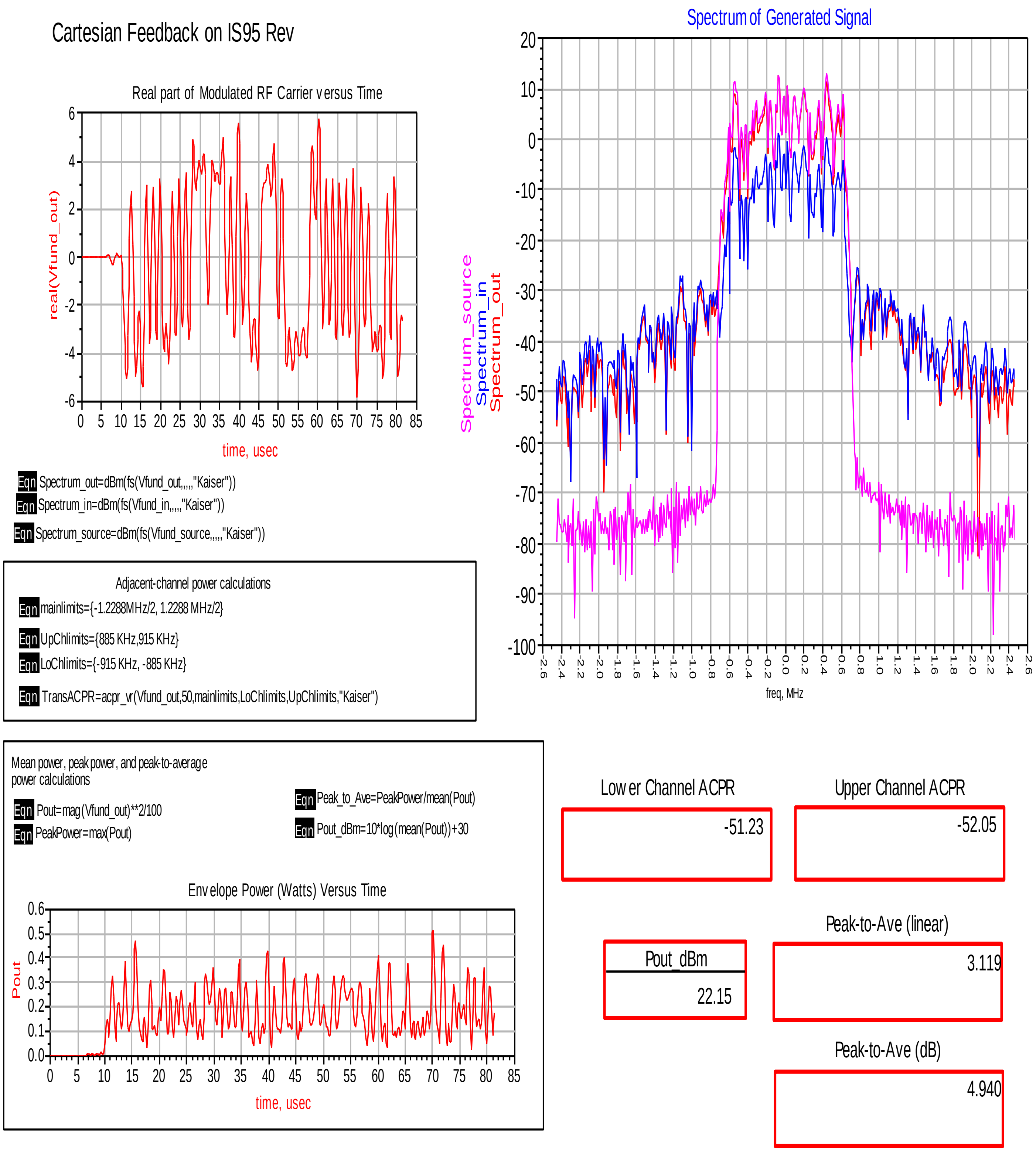

Figure 12. Closed loop.

systems were reviewed. OFDM is a very attractive technique for wireless communication due to its spectrum efficiency and channel robustness. One of the serious drawbacks in OFDM systems is that the transmit

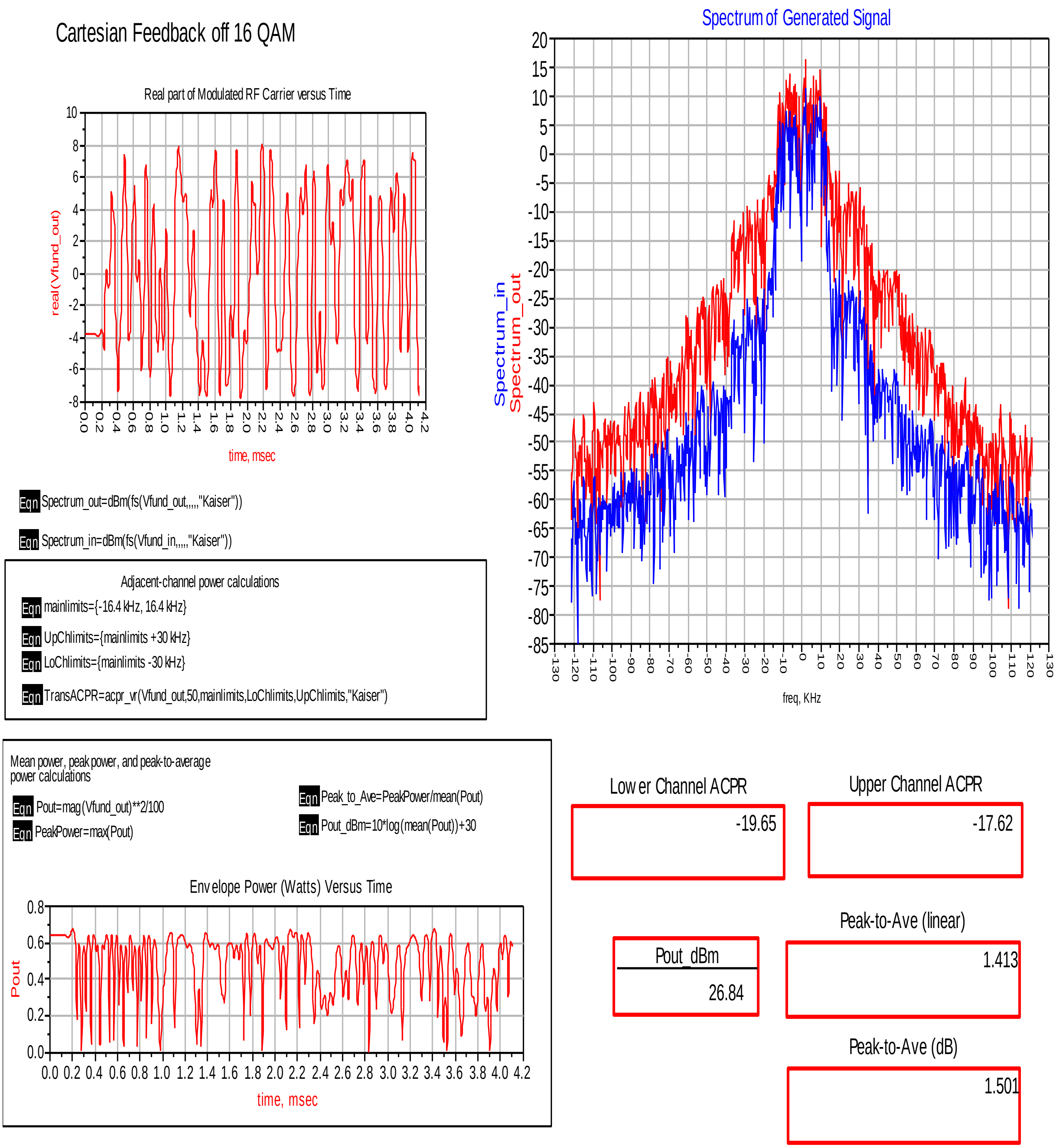

Figure 13. 16 QAM loop.

signal can exhibit a very high PAPR. In this paper, we have described several techniques to reduce PAPR in OFDM systems all of which have the potential to provide substantial reduction in PAPR at the cost of loss in data rate, signal power increase ,BER performance degradation, computational complexity

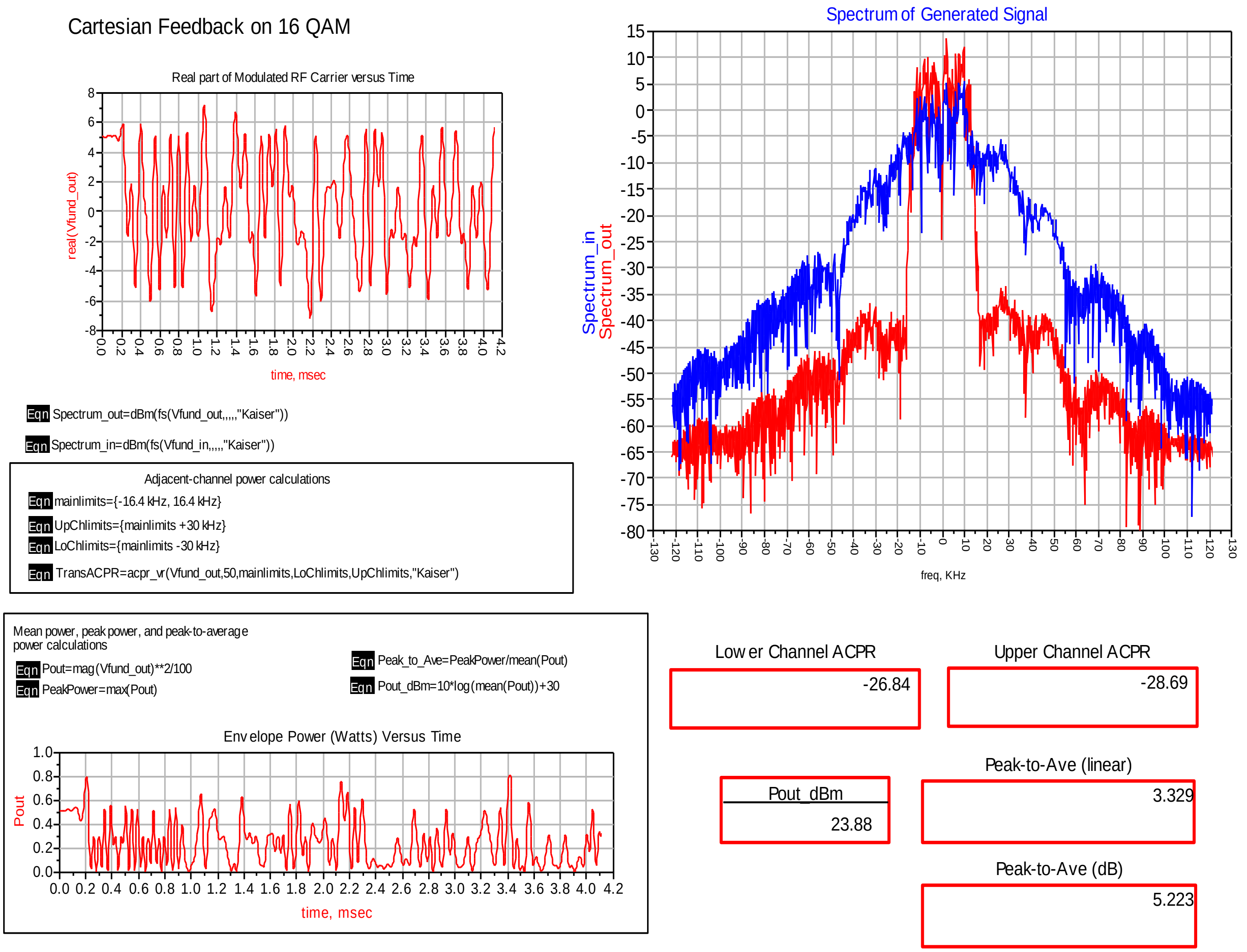

Figure 14. 16 QAM Closed loop.

increase, and so on. Therefore, the PAPR reduction technique should be carefully chosen according to various system requirements.

REFERENCES

Armstrong J (2002). Peak-to-average power reduction for OFDM by repeated clipping and frequency-domain Filtering." Elect. Lett., 38: 246-247.

Davis J, Jedwab J (1997). Peak-to-mean power control and error correction for OFDM transmission using Golay sequences and Reed-Muller codes." Elect. Lett., 33(4): 267-268.

Davis J, Jedwab J (1999). Peak-to-mean power control in OFDM, Golay complementary sequences and Reed-Muller codes." IEEE Trans. Inf. Theory, 45(7): 2397-2417.

Golay M (1961). Complementary series." IEEE Trans. Inf. Theory, 7: 82-87.

Han S, Lee J (2004). PAPR reduction of OFDM signals using a reduced complexity PTS technique." IEEE Sig. Proc. Lett., 11: 887-890.

Jones A, Wilkinson T (1996). Combined coding error control and increased robustness to system nonlinearities in OFDM." In Proc. IEEE 46th VTC 1996, Atlanta, Georgia, pp. 904-908.

Jones A, Wilkinson T, Barton S (1994). Block coding scheme for reduction of peak to mean envelope power ratio of multicarrier transmission schemes." Electron. Lett., 30: 2098-2099.

Li X, Cimini LJ (1998). Effects of clipping and Filtering on the performance of OFDM. 'IEEE Commun. Lett., 2: 131-133.

Ochiai H, Imai H (2000). Performance of the deliberate clipping with adaptive symbol selection for strictly band-limited OFDM systems. IEEE J. Select. Areas Commun., 18: 2270-2277.

Ochiai H, Imai H (2002). Performance analysis of deliberately clipped OFDM signals." IEEE Trans. Commun., 50(1): 89-101.

O'Neill R, Lopes L (1995). Envelope variations and spectral splatter in clipped multicarrier signals." In Proc. IEEE PIMRC 1995, Toronto, Canada, pp. 71-75.

Paterson K (2000). Generalized Reed{Muller codes and power control in OFDM modulation." IEEE Trans. Inf. Theory, 46(1): 104-120.

Popovic B (1991). Synthesis of power e±cient multitone signals with flat amplitude spectrum." IEEE Trans. Commun., 39: 1031-1033.

Sharif M, Gharavi-Alkhansari M, Khalaj B (2003). On the peak-to-average power of OFDM signals based on oversampling.' IEEE Trans. Commun., 51(1): 72-78.

Sharif M, Khalaj B (2001). Peak to mean envelope power ratio of oversampled OFDM signals: An analytical approach." In Proc. IEEE Int. Conf. Commun. (ICC), St. Petersburg, Russia, 5: 1476-1480.

Tarokh V, Jafarkhani H (2000). On the computation and reduction of the peak-to-average power ratio in multicarrier communications." IEEETrans. Commun., 48: 37-44.

Tarokh V, Jafarkhani H (2000). On the computation and reduction of the peak-to-average power ratio in multicarrier communications." IEEE Trans. Commun., 48: 37-44.